

Chemical Science

Accepted Manuscript



This is an *Accepted Manuscript*, which has been through the Royal Society of Chemistry peer review process and has been accepted for publication.

Accepted Manuscripts are published online shortly after acceptance, before technical editing, formatting and proof reading. Using this free service, authors can make their results available to the community, in citable form, before we publish the edited article. We will replace this *Accepted Manuscript* with the edited and formatted *Advance Article* as soon as it is available.

You can find more information about *Accepted Manuscripts* in the [Information for Authors](#).

Please note that technical editing may introduce minor changes to the text and/or graphics, which may alter content. The journal's standard [Terms & Conditions](#) and the [Ethical guidelines](#) still apply. In no event shall the Royal Society of Chemistry be held responsible for any errors or omissions in this *Accepted Manuscript* or any consequences arising from the use of any information it contains.

ARTICLE

Electronic Infrared Light Absorption of Tri-palladium Complex Containing Two π -Expanded Tetracene Ligands

Cite this: DOI: 10.1039/x0xx00000x

Received 00th January 2012,
Accepted 00th January 2012

DOI: 10.1039/x0xx00000x

www.rsc.org/Tsuyoshi Suzuki,^a Takafumi Nakagawa,^a Kei Ohkubo,^b Shunichi Fukuzumi,^b and Yutaka Matsuo*^a

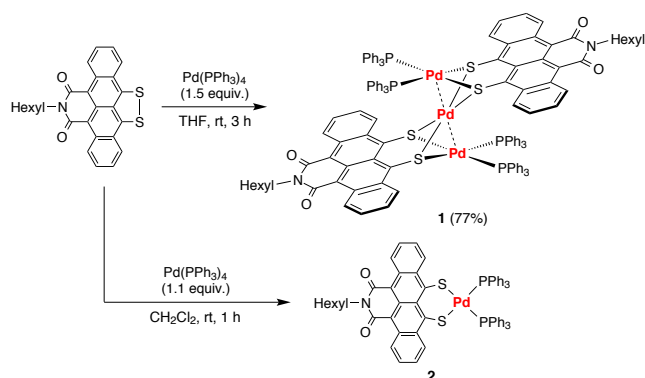
A large π -electron conjugated system consisting of bridging three palladium metals and two π -expanded tetracene derivatives was synthesized to have a narrow HOMO–LUMO gap for long-wavelength light absorption. The product, Pd₃(TIDS)₂(PPh₃)₄ (TIDS = narrow HOMO–LUMO gap tetracene ligand) showed far long-wavelength light absorption reaching the infrared region (absorption maximum = 1,982 nm, $\epsilon = 4.0 \times 10^4 \text{ M}^{-1} \text{ cm}^{-1}$ in CH₂Cl₂ solution; 2,500 nm in solid state). X-ray crystallography revealed the tri-metallic structure composed of three square-planar Pd coordination planes. The total oxidation number of the three Pd atoms is +4. Quantum chemical calculation was used to elucidate wholly delocalized π -conjugation in the non-coplanar structure and HOMO–LUMO transition for this unique absorption band. Time-resolved flash photolysis exhibited the excited state dynamics characterized with a triplet excited state (lifetime = 400 ps, $\lambda_{\text{max}} = 1,280 \text{ nm}$). A mononuclear Pd complex, Pd(TIDS)(PPh₃)₂ was also synthesized as a reference compound, and characterized with spectroscopic and X-ray crystallographic analyses.

Introduction

Long-wavelength light absorption and large molar absorption coefficient—unique characteristics of expanded π -electron conjugated compounds have attracted chemists to develop various photo-functional materials. This has led to producing numerous π -expanded compounds such as functionalized porphyrinoids,¹ perylene dyes,² acene analogues,³ and so on, toward organic electronic devices,⁴ bio-imaging labels,⁵ and chemosensors⁶ applications. In addition, chemists have tried a different approach to realize long-wavelength light absorption, that is, the use of transition metal atoms utilizing interaction between metallic $d\pi$ and organic $p\pi$ orbitals. One example is a metal bis(dithiolene) complex, in which a transition metal atom bridges laterally two organic π -conjugated units to have a narrow HOMO–LUMO gap.⁷ Another example is a multiple-decker phthalocyanine that has longitudinally alternative stacking of metals and phthalocyanines.⁸ These studies suggest that the metal-bridging method have great potential to create functional light-absorbing materials. Such kind of researches on π -extended metal complexes have, however, been less explored, compared with a fevered research for π -expanded organic compounds.⁹

In our recent work, we synthesized a π -expanded tetracene derivative, tetracene imide disulfide (TIDS) bearing electron-

withdrawing and -donating groups for lowering LUMO and raising HOMO levels, respectively, to have narrow HOMO–LUMO gap for long-wavelength light absorption (up to 850 nm, offset).¹⁰ We then examined complexation of an *N*-(*n*-hexyl)-substituted TIDS (HexylTIDS) ligand through oxidative addition¹¹ with a platinum atom to obtain a mononuclear platinum complex, Pt(HexylTIDS)(PPh₃)₂, which showed long-wavelength light absorption extended to 950 nm.¹² Herein, we report the synthesis, characterization, computational investigation, and time-resolved photophysical study of a trinuclear palladium complex as well as a prototype mononuclear palladium complex. The isolated palladium trinuclear complex electronically absorbed long-wavelength light extended to the infrared region with absorption peaks at 1,982 nm in solution and 2,500 nm in solid state. This unique absorption band is due to HOMO–LUMO transition with a wholly delocalized π -conjugated system.



Scheme 1 Synthesis of the trinuclear (**1**) and mononuclear palladium complexes (**2**).

Results and discussion

Synthesis and characterization of the tri-palladium bis(HexylTIDS) π -conjugated system.

The reaction of HexylTIDS with 1.5 equiv. of Pd(PPh₃)₄ in THF at room temperature for 3 h produced a trinuclear palladium complex Pd₃(HexylTIDS)₂(PPh₃)₄ (**1**) as black crystals (Scheme 1). The appearance of the reaction mixture changed from blue suspension to dark-red solution. Trinuclear complex **1** was purified by recrystallization in CH₂Cl₂/*n*-hexane in 77% yield. The single crystal X-ray analysis unambiguously revealed its trimetallic structure (Fig. 1, S1 and S2). Additionally, complex **1** was characterized by spectroscopic measurements, elemental analysis, and electrochemical studies. In the cyclic voltammetry, we observed three reversible reduction waves at $E_{1/2} = -0.50$ V, -0.76 V, -1.12 V vs. Fc/Fc⁺ in CH₂Cl₂ (Fig. 2 and S3). These reduction potentials of **1** were much positively shifted compared with those of the TIDS ligand ($E_{1/2} = -1.21$ V)¹⁰ and the mononuclear Pt-TIDS complex ($E_{1/2} = -1.45$ V).¹² Oxidation peak was not detected, even after considerable cyclic voltammetric measurements with different conditions using various solvents and working electrodes.

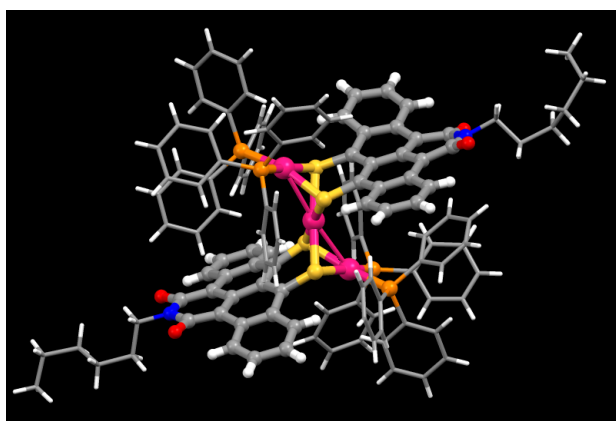


Fig. 1 X-ray crystallographic structure of **1**. The phenyl and hexyl groups are drawn with thin sticks. Solvent molecules (CH₂Cl₂) are omitted for clarity.

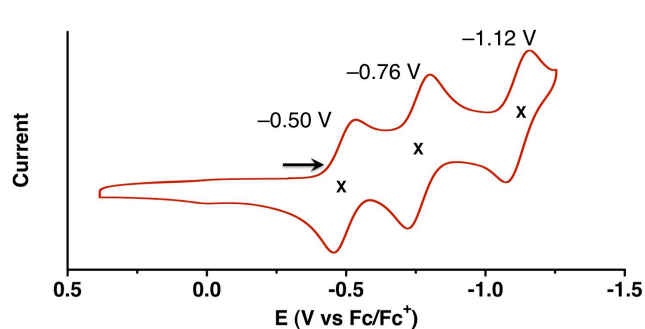


Fig. 2 Electrochemical properties of **1**. Conditions of cyclic voltammetry: solvent, CH₂Cl₂; concentration, 5.0×10^{-4} M; scan rate, 100 mV/s; working electrode, glassy carbon.

By modifying the synthetic method, a mononuclear complex Pd(HexylTIDS)(PPh₃)₂ (**2**) was synthesized as a reference compound. Separately prepared CH₂Cl₂ solutions of HexylTIDS and Pd(PPh₃)₄ were slowly mixed at room temperature instead of using THF suspension of HexylTIDS. The blue HexylTIDS solution and the yellow Pd(PPh₃)₄ solution reacted to give black solution of **2**. Characterization and X-ray crystal structure of **2** was noted in the latter section.

According to the X-ray crystal structural analysis of **1**, two square planar mononuclear Pd(HexylTIDS)(PPh₃)₂ units are connected by a central palladium atom, and the three palladium atoms are linearly aligned in this structure (Fig. 1). Distances between the two palladium atoms are 2.8818(5) and 2.9241(5) Å, which are longer than the Pd–Pd metallic bond distance (2.76 Å) but shorter than the sum of the two Van der Waals radii of palladium (3.26 Å), suggesting there are weak Pd···Pd interactions (see natural bond orbital analysis in the latter section). In comparison with linearly aligned trinuclear palladium complexes reported in the literatures,¹³ the observed Pd···Pd distances in complex **1** are close to those in a dithiadiazolyl palladium complex (Pd···Pd = 2.86 Å).¹⁴ Each HexylTIDS ligand in **1** bridges two palladium atoms like the reported naphthalene-dithiolate dinuclear complexes.¹⁵ The trinuclear structure of **1** is formally isoelectronic to the reported multimetallic Pt(II)···Ag(I)···Pt(II) complex having two naphthalene dithiolate ligands.¹⁶ A major difference between **1** and the silver(I) complex is the distance between metal atoms. Compound **1** has *ca.* 0.3-Å shorter Pd···Pd distance than the distance between Ag(I) and Pt(II) of the reported compound (3.0739(13), 3.2044(13) Å). Though the literature did not discuss about light absorption properties, the difference of metal-to-metal distances would afford a critical effect on the π -conjugated structure and photophysical properties.

The NMR signals of **1** were observed and there was no signal in ESR measurement (Fig. S4), indicating this complex does not contain paramagnetic Pd(I) species. The central palladium atom can be considered as Pd(0) with an 18-electron configuration, sandwiched between two mononuclear complexes **2** that have a 16-electron configuration at the Pd(II) center.

In the UV-vis-NIR absorption spectrum of **1**, two intense absorption bands were observed around at 922 nm ($\epsilon = 2.1 \times$

$10^4 \text{ M}^{-1} \text{ cm}^{-1}$) and 1,982 nm (0.626 eV) with large absorption coefficient ($\epsilon = 4.0 \times 10^4 \text{ M}^{-1} \text{ cm}^{-1}$) (Fig. 3a), while the absorption peak of HexylTIDS in the longest wavelength is at 784 nm. In the IR absorption spectrum measured in the solid state, a broad absorption peak was observed in the infrared region with a maximum at 2,500 nm (0.496 eV, $4,000 \text{ cm}^{-1}$) (Fig. 3b). Because we usually do not observed such a broad peak in this region in the IR spectra, we assigned this peak to the same electronic transition observed in the solution. Observed 0.13-eV shift to small energy is attributable to electronic interaction between the molecules in the solid state. The extended absorption range and enhanced absorption coefficient indicate the existence of a massively extended π -conjugated system (vide infra). The highest absorption coefficient of **1** is almost twice of that of $\text{Pt}(\text{HexylTIDS})(\text{PPh}_3)_2$ at 843 nm ($\epsilon = 2.2 \times 10^4 \text{ M}^{-1} \text{ cm}^{-1}$).¹² This is reasonable because **1** contains two mono-metallic **2** moieties.

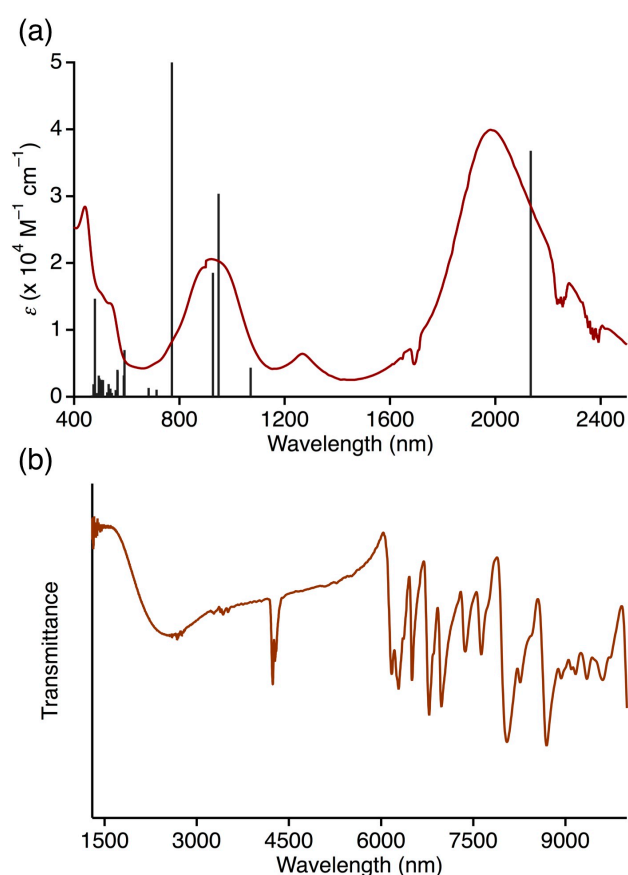


Fig. 3 Absorption spectra of **1**. (a) UV-vis-NIR spectrum and simulated absorption bands calculated at the B3LYP/SDD/6-31G(d) level. The spectrum was measured in CH_2Cl_2 . (b) IR spectrum. A broad electronic absorption maximum was observed at $4,000 \text{ cm}^{-1}$ (2,500 nm)

Theoretical calculations for the tri-palladium bis(HexylTIDS) π -conjugated system.

To gain further insight into the light absorption properties of **1**, we performed DFT calculation of a simplified methyl-substituted model analogue ($\text{Pd}_3(\text{MeTIDS})_2(\text{PPh}_3)_4$) (**3**) (Fig. S5). The optimized structures are almost identical to the

structure of **1** obtained by X-ray crystallography (See Electronic Supplementary Information). As shown in the Fig. 1, the π -orbitals of the TIDS ligands are bound in parallel but lie in different planes. Nevertheless, the theoretical calculation showed that the HOMO and LUMO of the model complex **3** are delocalized on the two TIDS ligands (Fig. 4), thus providing a narrow HOMO–LUMO gap (0.68 eV). The TD-DFT calculation (Fig. S6) for light absorption simulation revealed that the strong absorption band observed at 1,982 nm mainly corresponds to a HOMO–LUMO transition, while the absorption band at 922 nm was assigned to charge-transfer (CT) band between the palladium atoms and the TIDS ligand. The parallel coordination of the ligands would be a key to bring the fully delocalized HOMO and LUMO even in the non-coplanar structure. Accordingly, thorough investigation of electronic structures in the HOMO and the LUMO is essential to cultivate a deep understanding of the photophysical properties of **1**.

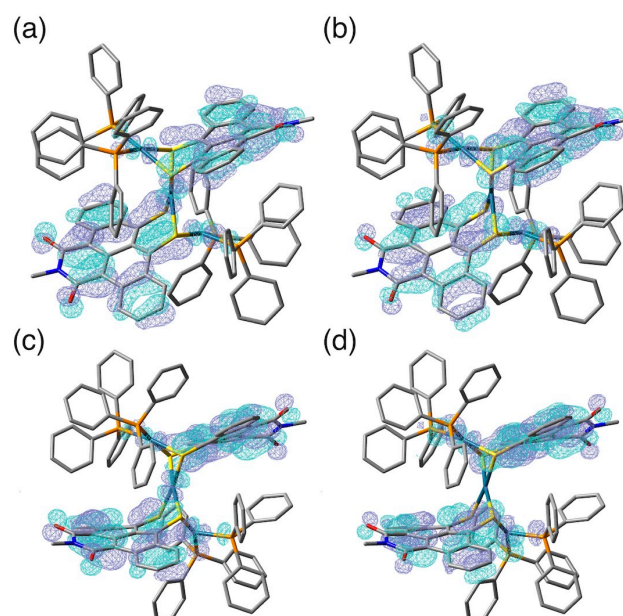


Fig. 4 Optimized structures and molecular orbitals of **3**. (a) HOMO. (b) LUMO. (c and d) HOMO and LUMO from different viewpoints. The calculations were performed at the B3LYP/SDD/6-31G(d) level.

The structures of HOMO and LUMO in **1** were successfully explained by molecular orbital interaction analysis (Fig. S8), which described how to construct the quite narrow HOMO–LUMO gap. For the analysis, $\text{Pd}_3(\text{MeTIDS})_2(\text{PPh}_3)_4$ molecule was divided into three subunits: two mononuclear palladium complex subunits $\text{Pd}(\text{MeTIDS})(\text{PPh}_3)_2$ like compound **2** and one central Pd. According to this analysis, we propose that the HOMO of **1** is composed of orbital interaction of HOMO of the central Pd (d_{xy} orbital) with LUMOs of $\text{Pd}(\text{MeTIDS})(\text{PPh}_3)_2$ (as seen in Fig. 4c); LUMO of **1** is derived from another LUMOs of $\text{Pd}(\text{MeTIDS})(\text{PPh}_3)_2$, giving narrow HOMO–LUMO gap (as seen in Fig. 4d).

The interactions between the central palladium atom and its peripheral atoms were further investigated by natural bond

orbital (NBO) analysis. The Wiberg bond indexes of Pd··Pd were 0.133 and 0.144 suggesting the presence of weak Pd··Pd interactions (Table S3). In addition, the central palladium is regarded as being more electron-rich than other palladium atoms (Table S4). This is in good agreement with our consideration for the oxidation numbers of palladium atoms in **1** as Pd(II)–Pd(0)–Pd(II).

Characterization of the mono-palladium HexylTIDS complex (**2**).

Different from **1**, complex **2** was not able to be purified because of the instability of **2** without free PPh₃. A UV-vis-NIR absorption spectrum of **2** in the presence of PPh₃ showed that absorption of **2** was almost consistent with that of the mononuclear platinum complex we previously reported (Fig. 5).¹² Complex **2** showed no infrared light absorption. TD-DFT calculation supported this experimental observation (Fig. S10).

In addition, after many attempts to recrystallize complex **2**, we obtained a crystal which was suitable for X-ray structural analysis (Fig. 6). The crystal structure of **2** showed a bending structure caused by the large radius of sulfur atoms and a square planar coordination mode of the palladium atom. The dihedral angle is *ca.* 46°, which is similar to those of Pd(HexylTIDS)(PPh₃)₂ moiety in **1** (55°, 47°). This bending structure provides a coordination site at the disulfide moiety to form trinuclear complex **1**.

DFT calculations for Pd(MeTIDS)(PPh₃)₂ revealed a delocalized π -orbital over the entirety of the molecule (Fig. 7). Here, mononuclear complex **2** did not show intense infrared absorption. The calculation represents that full π -conjugation over mono-metallic moiety is not enough to show infrared absorption. Consequently, the two mono-metallic subunit Pd(HexylTIDS)(PPh₃)₂ in **1** should be π -conjugated through the central palladium atom to extend the light absorption range up to the infrared region. In other words, the narrow HOMO–LUMO gap and electronic infrared light absorption of **1** are concluded to arise from the π -orbitals of the two HexylTIDS units being linked through three palladium atoms.

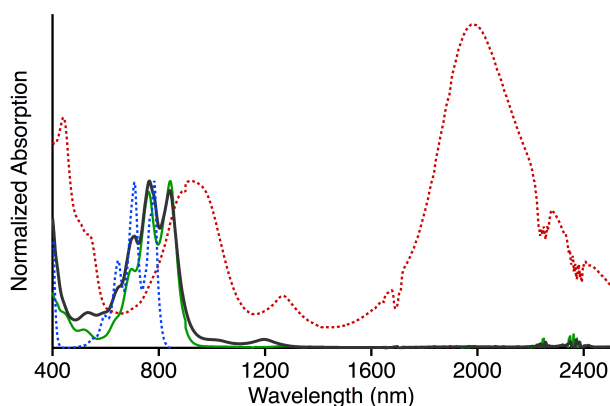


Fig. 5 Normalized UV-vis-NIR absorption spectra of HexylTIDS (blue dot), mononuclear complex **2** with triphenylphosphine (black solid line), trinuclear complex **1** (red dot) and Pt(HexylTIDS)(PPh₃)₂ (green solid line).

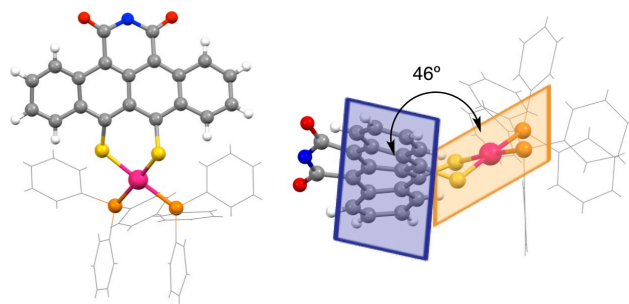


Fig. 6 Crystal structures of the mononuclear **2**.

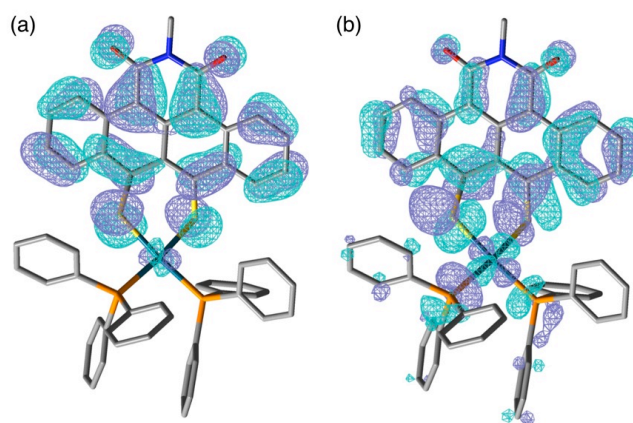


Fig. 7 Optimized structures and of the mononuclear Pd(MeTIDS)(PPh₃)₂ calculated at the B3LYP/LANL2DZ/6-31G(d) level. (a) HOMO and (b) LUMO.

Time-resolved photophysical characterization for the tri-palladium bis(TIDS) π -conjugated system.

Finally, we characterized the photoexcited state of the tri-palladium complex **1**. To investigate excited state of **1** in the photoinduced processes, we conducted femtosecond time-resolved transient absorption measurements of **1** in the vis-NIR region by photoexcitation at 800 nm (Fig. 8). This wavelength is in the shoulder of the CT absorption band ($\lambda_{\text{max}} = 922$ nm); laser instrument for excitation at *ca.* 2,000 nm was unavailable. The spectra measured in THF displayed prompt increases in absorption bands at 480, 580 and 1,080 nm with ground-state bleaching band at 970 nm (black line in Fig. 8). Then, the absorption band at 1,080 nm decreased quickly, accompanied by the appearance of a new near-infrared absorption at 1,280 nm with an isosbestic point at 1,200 nm with a rate constant of $1.1 \times 10^{11} \text{ s}^{-1}$ (Fig. 9). These characteristics strongly suggest that the singlet CT state corresponding to the peak at 1,080 nm was converted by intersystem crossing to form the triplet CT state corresponding to the peak at 1,280 nm. The lifetime of the singlet CT state was determined to be 9 ps. The triplet CT lifetime was determined from the decay of the absorption band

at 1,280 nm to be 400 ps [= $(2.5 \times 10^9 \text{ s}^{-1})^{-1}$]. In contrast, HexylTIDS does not show any transient absorption peak corresponding to a triplet state.¹² Moreover, the lifetime of the triplet state in **1** is relatively short, indicating that the forbidden relaxation process $S_0 \leftarrow T_1$ is also accelerated by the heavy atom effect. The transient absorption was measured in toluene as well (Fig. S11). The kinetic constants calculated from the time-dependent changes of the singlet and triplet peaks ($1.2 \times 10^{11} \text{ s}^{-1}$, $3.7 \times 10^9 \text{ s}^{-1}$) are slightly larger than those in THF (Fig. S12). The small dependence of the rate constants on solvent polarity implies that the excited states have small polarities because of the symmetric molecular structure and the symmetrically delocalized π -orbitals.

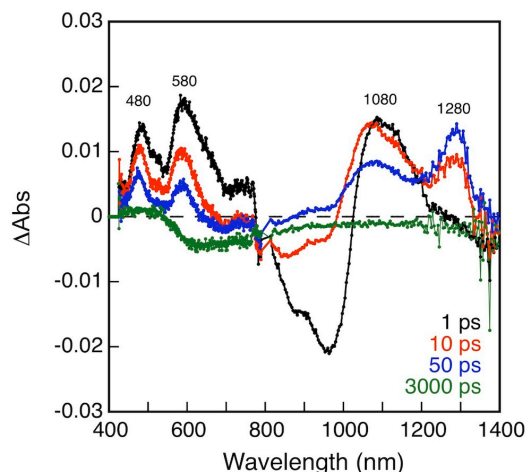


Fig. 8 Transient absorption spectra of **1** in THF after femtosecond laser excitation ($\lambda = 800 \text{ nm}$) at 1, 10, 50, and 3000 ps.

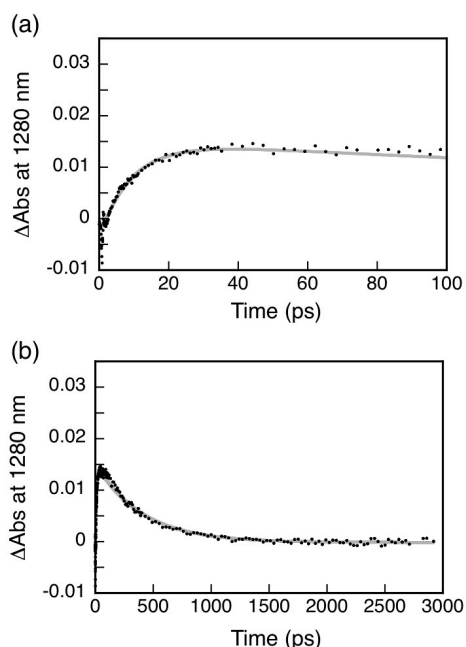


Fig. 9 Time-dependent profile of an absorption peak at 1280 nm in the transient absorption spectra shown in Fig. 7.

Conclusions

In summary, we have demonstrated the construction of a large $d\pi/p\pi$ -conjugated systems by tri-palladation of the TIDS ligands. The obtained tri-palladium complex showed electronic infrared light absorption at 1,982 nm with a high absorption coefficient ($\epsilon = 4.0 \times 10^4 \text{ M}^{-1} \text{ cm}^{-1}$) in CH_2Cl_2 solution as well as at 2,500 nm in the solid state. In contrast, mono-metallic palladium complex with one HexylTIDS ligand mainly absorbs visible and near-IR region. With quantum chemical calculation, we found that the origin of the intense infrared light absorption is HOMO–LUMO transition at entirely delocalized HOMO and LUMO. The d-orbitals of palladium atoms connect two HexylTIDS ligands in a non-coplanar parallel fashion to form a large π -conjugated system. In addition, the triplet excited state (lifetime = 400 ps, $\lambda_{\text{max}} = 1,280 \text{ nm}$) of the trinuclear palladium complex was characterized by femtosecond laser flash photolysis. The present work suggests the applicability of trimetallic connection for bridging organic π -conjugated systems to construct narrow HOMO–LUMO gap materials for long-wavelength light absorption. This achievement would provide a new design concept of functional organic dyes used in various applications.

Experimental section

General

All NMR spectra were taken at 500 MHz (JEOL ECA-500 spectrometer). NMR spectra were recorded in parts per million (ppm, δ scale) from residual protons of the CD_2Cl_2 for ^1H NMR (δ 5.32 ppm for dichloromethane) and from an external standard for ^{31}P NMR (δ 29.41 ppm of OPPh_3 for all solvents). The CD_2Cl_2 was distilled with CaH_2 prior to use and stored under argon with molecular sieves (4 Å). The data were presented as following space: chemical shift, multiplicity ($s =$ singlet, $d =$ doublet, $t =$ triplet, $m =$ multiplet and/or multiplet resonances, $br =$ broad), coupling constant in hertz (Hz), and signal area integration in natural numbers, assignment (*italic*). Elemental analysis was performed at the University of Tokyo, Department of Chemistry, Organic Elemental Analysis Laboratory. IR absorption was measured on JASCO FT/IR-6100 equipped with an attenuated total reflection (ATR) with ZnSe, and was reported as wavenumber in cm^{-1} .

Synthesis of $\text{Pd}_3(\text{HexylTIDS})_2(\text{PPh}_3)_4$ (**1**).

A mixture of HexylTIDS (100 mg, 0.225 mmol) and $\text{Pd}(\text{PPh}_3)_4$ (391 mg, 0.338 mmol, 1.50 equiv.) was stirred in THF (6.6 mL) at room temperature for 3 h. The *n*-hexane was added to precipitate the crude product, which was purified by crystallization from $\text{CH}_2\text{Cl}_2/n$ -hexane to give dark-red crystals

in 77% yield (196 mg, 0.0869 mmol). ^1H NMR (400 MHz, CD_2Cl_2): δ = 9.37 (br, tetracene), 7.41 (br, tetracene), 6.99 (t, J = 7.3 Hz, 4H, *p*-Ph), 6.81–6.73 (m, 16H, *o*-Ph, *m*-Ph), 6.11 (br, tetracene), 4.26 (t, J = 6.9 Hz, 4H, CH_2 in hexyl), 1.99–1.92 (m, 4H, CH_2 in hexyl), 1.62–1.54 (m, 4H, CH_2 in hexyl), 1.38–1.51 (m, 8H, CH_2CH_2 in hexyl), 0.95 (t, J = 7.1 Hz, 6H, Me in hexyl). Anal. calcd for $\text{C}_{124}\text{H}_{102}\text{N}_2\text{O}_4\text{Pd}_3\text{S}_4$: C, 66.03; H, 4.56; N, 1.24. Found: C, 66.13; H, 4.71; N, 1.14.

^1H NMR peaks corresponding to tetracene moiety were broadened at room temperature. This would be resulted from the thermal dynamic behavior. According to the same reason, neither ^{31}P nor ^{13}C NMR were clearly recorded. Low temperature ^1H NMR measurement even at -30 °C exhibited broaden peaks.

Synthesis of Pd(HexylTIDS)(PPh_3)₂ (2).

$\text{Pd}(\text{PPh}_3)_4$ (127 mg, 0.110 mmol, 1.1 equiv.) in CH_2Cl_2 (6.5 mL) was added dropwise to a solution of HexylTIDS (44.5 mg, 0.100 mmol) in CH_2Cl_2 (20 mL) for 25 min. The appearance of the solution changed from blue suspension to black solution. It was stirred at room temperature for 1 h. This solution was used for each analysis. ^1H NMR (500 MHz, CD_2Cl_2): δ = 9.81 (d, J = 9.2 Hz, 2H, tetracene), 8.45 (d, J = 9.2 Hz, 2H, tetracene), 7.57–7.54 (m, 2H, tetracene), 7.43 (t, J = 7.5 Hz, 6H, *p*-Ph), 7.27–7.24 (m, 12H, *o*-Ph, *m*-Ph), 7.12–7.08 (m, 2H, tetracene), 4.28 (t, J = 7.7 Hz, 2H, CH_2 in hexyl), 1.80–1.74 (m, 2H, CH_2CH_2 in hexyl), 1.48–1.44 (m, 2H, CH_2 in hexyl), 1.40–1.31 (m, 4H, CH_2CH_2 in hexyl), 0.90 (t, J = 7.2 Hz, 3H, Me in hexyl). ^{31}P NMR (202.4 MHz, CD_2Cl_2): δ = 27.66 (s, 2P, PPh_3).

Electrochemical analysis.

Cyclic voltammetry (CV) and differential pulse voltammetry (DPV) were performed using HOKUTO DENKO HZ-5000 voltammetric analyzer. All CV measurements were carried out in a one-compartment cell under argon gas, equipped with a glassy-carbon working electrode, a platinum wire counter electrode, and an Ag/Ag^+ reference electrode. The supporting electrolyte was a 0.1 mol/L dichloromethane solution of tetrabutylammonium hexafluorophosphate (TBAPF_6). Only for the CV measurements of tri-palladium complex **1**, platinum and gold working electrode were additionally used to result in the identical CV charts to that obtained with glassy-carbon electrode. The electrochemical data equipped with a glassy-carbon working electrode are presented in this report.

X-ray crystallographic analysis.

X-ray crystallographic analyses for complexes **1** and **2** were performed using a RIGAKU R-Axis RAPID II (imaging plate detector) with monochromic $\text{CuK}\alpha$ (λ = 1.5406 Å) radiation. The positional and thermal parameters were refined by a full-matrix least-squares method using the SHELXL97 program on the Yadokari-software. The CCDC numbers of complexes **1** and **2** were 881159 and 978047, respectively.

Computational Studies.

All calculations were carried out by Gaussian09 package at the B3LYP level. Palladium atoms were represented by the LANL2DZ or SDD basis set and a 6-31G(d) basis set was used for other atoms (C, H, N, O, S, and P). The calculation levels are described as “B3LYP/LANL2DZ/6-31G(d)” and “B3LYP/SDD/6-31G(d)”.

Time-resolved Transient Absorption Measurements.

Femtosecond transient absorption spectroscopy experiments were conducted using an ultrafast Integra-C (Quantronix Corp.), a TOPAS optical parametric amplifier (Light Conversion Ltd.), and a commercially available Helios optical detection system provided by Ultrafast Systems LLC.

Acknowledgements

This work was supported by the Funding Program for Next-Generation World-Leading Researchers (Y.M.), and the Advanced Leading Graduate Course for Photon Science (T.S.). The computations were performed at the Research Center for Computational Science, Okazaki, Japan.

Notes and references

^a Department of Chemistry, School of Science, The University of Tokyo, 7-3-1 Hongo, Bunkyo-ku, Tokyo 113-0033, Japan

^b Department of Material and Life Science, Graduate School of Engineering, Osaka University, ALCA (JST), Suita, Osaka 565-0871, Japan

^c Address here.

† Electronic Supplementary Information (ESI) available: data for X-ray crystallography, light absorption, ESR, electrochemistry, DFT calculation and flash photolysis. See DOI: 10.1039/b000000x/

- (a) I. M. Blake, L. H. Rees, T. D. W. Claridge and H. L. Anderson, *Angew. Chem. Int. Ed.*, 2000, **39**, 1818–1821. (b) A. Tsuda and A. Osuka, *Science*, 2001, **293**, 79–82. (c) K. Kurotobi, K. S. Kim, S. B. Noh, D. Kim and A. Osuka, *Angew. Chem. Int. Ed.*, 2006, **45**, 3944–3947. (d) N. K. S. Davis, A. L. Thompson and H. L. Anderson, *J. Am. Chem. Soc.*, 2011, **133**, 30–31. (e) T. Sarma and P. K. Panda, *Chem. Eur. J.*, 2011, **17**, 13987–13991.
- (a) Y. Avlasevich and K. Müllen, *Chem. Commun.*, 2006, 4440–4442. (b) N. G. Pshirer, C. Kohl, F. Nolde, J. Qu and K. Müllen, *Angew.*

- Chem. Int. Ed.*, 2006, **45**, 1401–1404. (c) M.-J. Lin, B. Fimmel, K. Radacki and F. Würthner, *Angew. Chem. Int. Ed.*, 2011, **50**, 10847–10850.
- 3 (a) L. Qiu, C. Yu, N. Zhao, W. Chen, Y. Guo, X. Wan, R. Yang and Y. Liu, *Chem. Commun.*, 2012, **48**, 12225–12227. (b) M. Nakao, H. Mori, S. Shinamura and K. Takimiya, *Chem. Mater.*, 2012, **24**, 190–198. (c) M. Más-Montoya, R. P. Ortiz, D. Curiel, A. Espinosa, M. Allain, A. Facchetti and T. J. Marks, *J. Mater. Chem. C*, 2013, **1**, 1959–1969. (d) T. Mori, T. Nishimura, T. Yamamoto, I. Doi, E. Miyazaki, I. Osaka and K. Takimiya, *J. Am. Chem. Soc.*, 2013, **135**, 13900–13913.
- 4 (a) H. E. Katz, Z. Bao and S. L. Gilat, *Acc. Chem. Res.*, 2001, **34**, 359–369. (b) M. Bendikov, F. Wudl and D. F. Perepichka, *Chem. Rev.*, 2004, **104**, 4891–4946. (c) J. E. Anthony, *Chem. Rev.*, 2006, **106**, 5028–5048. (d) K. Takimiya, I. Osaka and M. Nakano, *Chem. Mater.*, 2014, **26**, 587–593.
- 5 (a) Y. Ma and Y. Wang *Coord. Chem. Rev.*, 2010, **254**, 972–990. (b) K. K.-W. Lo, K. Y. Zhang and S. P.-Y. Li, *Eur. J. Inorg. Chem.*, 2011, 3551–3568. (c) S. Yao and K. D. Belfield, *Eur. J. Org. Chem.*, 2012, 3199–3127.
- 6 (a) T. Gunnlaugsson, M. Glynn, G. M. Tocci, P. E. Kruger and F. M. Pfeffer, *Coord. Chem. Rev.*, 2006, **250**, 3094–3117. (b) E. M. Nolan and S. J. Lippard, *Chem. Rev.*, 2008, **108**, 3443–3480. (c) J. J. Bryant and U. H. F. Bunz, *Chem. Asian J.*, 2013, **8**, 1354–1367. (d) X. Li, X. Gao, W. Shi and H. Ma, *Chem. Rev.*, 2014, **114**, 590–659.
- 7 (a) U. T. Mueller-Westerhoff, B. Vance and D. I. Yoon, *Tetrahedron*, 1991, **47**, 909–932. (b) A. Kobayashi, M. Sasa, W. Suzuki, E. Fujiwara, H. Tanaka, M. Tokumoto, Y. Okano, H. Fujiwara and H. Kobayashi, *J. Am. Chem. Soc.*, 2004, **126**, 426–427. (c) V. Madhu and S. K. Das, *Inorg. Chem.*, 2008, **47**, 5055–5070. (d) S. Dalglish, M. M. Matsushita, L. Hu, B. Li, H. Yoshikawa and K. Awaga, *J. Am. Chem. Soc.*, 2012, **134**, 12742–12750.
- 8 (a) N. Ishikawa, T. Okubo and Y. Kaizu, *Inorg. Chem.*, 1999, **38**, 3173–3181. (b) T. Fukuda, T. Biyajima and N. Kobayashi, *J. Am. Chem. Soc.*, 2010, **132**, 6278–6279. (c) T. Fukuda, W. Kuroda and N. Ishikawa, *Chem. Commun.*, 2011, **47**, 11686–11688. (d) H. Wang, K. Qian, K. Wang, Y. Bian, J. Jiang and S. Gao, *Chem. Commun.*, 2011, **47**, 9624–9626. (e) H. Wang, N. Kobayashi and J. Jiang, *Chem. Commun.*, 2012, **18**, 1047–1049. (f) T. Fukuda, K. Hata and N. Ishikawa, *J. Am. Chem. Soc.*, 2012, **134**, 14698–14701. (g) T. Fukuda, K. Matsumura and N. Ishikawa, *J. Phys. Chem. A*, 2013, **117**, 10447–10454.
- 9 (a) M. D. Watson, A. Fechtenkötter and K. Müllen, *Chem. Rev.*, 2001, **101**, 1267–1300. (b) K. Kawasumi, Q. Zhang, Y. Segawa, L. T. Scott and K. Itami, *Nat. Chem.*, 2013, **5**, 739–744.
- 10 (a) T. Okamoto, T. Suzuki, H. Tanaka, D. Hashizume and Y. Matsuo, *Chem. Asian J.*, 2012, **7**, 105–111. (b) T. Suzuki, T. Okamoto, A. Saeki, S. Seki, H. Sato and Y. Matsuo, *ACS Appl. Mater. Interfaces*, 2013, **5**, 1937–1942. (c) S. Kojima, T. Okamoto, K. Miwa, H. Sato, J. Takeya and Y. Matsuo, *Org. Electron.*, 2013, **14**, 437–444.
- 11 (a) W. P. Bosman and H. G. M. van der Linden, *J. Chem. Soc. Chem. Commun.*, 1977, 714–815. (b) A. W. Gal, J. W. Gosselink and F. A. Vollenbroek, *Inorg. Chim. Acta*, 1979, **32**, 235–241. (c) S. M. Aucott, H. L. Milton, S. D. Robertson, A. M. Z. Slawin, G. D. Walker and J. D. Woollins, *Chem. Eur. J.*, 2004, **10**, 1666–1676.
- 12 T. Nakagawa, T. Suzuki, M. König, D. M. Guldi and Y. Matsuo, *Chem. Commun.*, 2013, **49**, 10394–10396.
- 13 (a) T. Murahashi, Y. Higuchi, T. Katoh and H. Kurosawa, *J. Am. Chem. Soc.*, 2002, **124**, 14288–14289. (b) M. Ohashi, J. Yi, D. Shimizu, T. Yamagata, T. Ohshima and K. Mashima, *J. Organomet. Chem.*, 2006, **691**, 2457–2464. (c) L. Brunet, F. Mercier, L. Ricard and F. Mathey, *Angew. Chem. Int. Ed. Engl.*, 1994, **33**, 742–745. (d) S. Kannan, A. J. James and P. R. Sharp, *J. Am. Chem. Soc.*, 1998, **120**, 215–216.
- 14 A. J. Banister, I. B. Gorrell, J. A. K. Howard, S. E. Lawrence, C. W. Lehman, I. May, J. M. Rawson, B. K. Tanner, C. I. Gregory, A. J. Blake and S. P. Fricker, *J. Chem. Soc., Dalton Trans.*, 1997, 377–384.
- 15 (a) H. Xu and J. H. K. Yip, *Inorg. Chem.*, 2003, **42**, 4492–4494. (b) S. M. Aucott, H. L. Milton, S. D. Robertson, A. M. Z. Slawin and J. D. Woollins, *Dalton Trans.*, 2004, 3347–3352. (c) A. P. S. Samuel, D. T. Co, C. L. Stern and M. R. Wasielewski, *J. Am. Chem. Soc.*, 2010, **132**, 8813–8815.
- 16 S. D. Robertson, A. M. Z. Slawin and J. D. Woollins, *Eur. J. Inorg. Chem.*, 2007, 247–253.